Earth and Planetary Science Letters 515 (2019) 231–247

Contents lists available at ScienceDirect

Earth and Planetary Science Letters

www.elsevier.com/locate/epsl

Daily bathymetric surveys document how stratigraphy is built and its extreme incompleteness in submarine channels

D. Vendettuoli [a,b,*], M.A. Clare [a], J.E. Hughes Clarke [c], A. Vellinga [a,b], J. Hizzet [a,b], S. Hage [a,d], M.J.B. Cartigny [d], P.J. Talling [d], D. Waltham [e], S.M. Hubbard [f], C. Stacey [g], D.G. Lintern [g]

[a] National Oceanography Centre, University of Southampton, Waterfront Campus, Southampton SO14 3ZH, UK
[b] Ocean and Earth Sciences, University of Southampton, Southampton SO14 3ZH, UK
[c] Center for Coastal and Ocean Mapping, University of New Hampshire, USA
[d] Durham University, Department of Geography and Earth Science, UK
[e] Royal Holloway University of London, Department of Earth Science, UK
[f] Department of Geoscience, University of Calgary, Calgary, Alberta T2N 1N4, Canada
[g] Geological Survey of Canada, Institute of Ocean Science, Canada

ARTICLE INFO

Article history:
Received 20 September 2018
Received in revised form 12 March 2019
Accepted 23 March 2019
Available online xxxx
Editor: J.P. Avouac

Keywords:
stratigraphic completeness
submarine channel
turbidity current
crescentic bedform
submarine landslide
channel-lobe transition zone

ABSTRACT

Turbidity currents are powerful flows of sediment that pose a hazard to critical seafloor infrastructure and transport globally important amounts of sediment to the deep sea. Due to challenges of direct monitoring, we typically rely on their deposits to reconstruct past turbidity currents. Understanding these flows is complicated because successive flows can rework or erase previous deposits. Hence, depositional environments dominated by turbidity currents, such as submarine channels, only partially record their deposits. But precisely how incomplete these deposits are, is unclear. Here we use the most extensive repeat bathymetric mapping yet of any turbidity current system, to reveal the stratigraphic evolution of three submarine channels. We re-analyze 93 daily repeat surveys performed over four months at the Squamish submarine delta, British Columbia in 2011, during which time >100 turbidity currents were monitored. Turbidity currents deposit and rework sediments into upstream-migrating bedforms, ensuring low rates of preservation (median 11%), even on the terminal lobes. Large delta-lip collapses (up to 150,000 m^3) are relatively well preserved, however, due to their rapidly emplaced volumes, which shield underlying channel deposits from erosion over the surveyed timescale. The biggest gaps in the depositional record relate to infrequent powerful flows that cause significant erosion, particularly at the channel-lobe transition zone where no deposits during our monitoring period are preserved. Our analysis of repeat surveys demonstrates how incomplete the stratigraphy of submarine channels can be, even over just 4 months, and provides a new approach to better understand how the stratigraphic record is built and preserved in a wider range of marine settings.

1. Introduction

It is important to understand how offshore sedimentary systems evolve, and the resultant stratigraphic architecture. For example, predicting this stratigraphic architecture is important for recovering oil and gas reserves, or when attempting to reconstruct past records of geohazards, such as submarine landslides or powerful gravity-driven sediment flows known as turbidity currents (Clark and Pickering, 1996; Carter et al., 2014). Stratigraphic architecture observed in seismic profiles, sediment cores and outcrops is typically used to reconstruct sedimentary system evolution; however, from these data we cannot tell what may have been deposited but not preserved (Hubbard et al., 2014; Durkin et al., 2018). Thus, we often rely upon forward numerical models to understand how architecture is built (Sylvester et al., 2011; Jobe et al., 2017). In subaerial environments, repeat satellite or aerial photogrammetry surveys enable monitoring of river and delta evolution, and thus calibration of these models (Moody and Meade, 2014; Schwenk et al., 2017). Such aerial techniques cannot image seaward of the shallow coastal zone, however. Therefore, laboratory experiments are used to understand how architecture is built and preserved in deep-sea sedimentary systems (e.g. Paola et al., 2009). These experiments are subject to scaling issues; hence, there is a pressing need for field-scale observations to under-

* Corresponding author at: National Oceanography Centre, University of Southampton, Waterfront Campus, Southampton SO14 3ZH, UK.
E-mail address: D.Vendettuoli@soton.ac.uk (D. Vendettuoli).

https://doi.org/10.1016/j.epsl.2019.03.033

stand the accuracy of such models and interpret geological archives (Talling et al., 2015).

1.1. Using repeat seafloor surveys to observe stratigraphic evolution of marine systems

Recent technological advances have enabled accurate bathymetric surveys to be collected repeatedly, to produce time-lapse data. These time-lapse surveys can provide a major advance in understanding of the rate and nature of seafloor change in different settings. Previous examples of marine time-lapse surveys include studies of estuaries (Mastbergen et al., 2016), submarine deltas (Hill et al., 2008; Casalbore et al., 2011; Biscara et al., 2012; Clare et al., 2017; Lintern et al., 2016), continental slopes (Kelner et al., 2016), deep-sea submarine canyons (Smith et al., 2007; Xu et al., 2008; Paull et al., 2018; Mountjoy et al., 2018), submarine channels in fjords (Conway et al., 2012; Normandeau et al., 2014; Gales et al., 2018), and lakes (Corella et al., 2016; Silva et al., 2018). These time-lapse datasets cover seven or fewer repeat surveys, over timescales of months to decades (Table S1), which is much less frequent than the rate at which sediment transport events occur. As a result, it has been challenging to document stratigraphic evolution in detail.

Here we analyze the most detailed time-lapse mapping yet of any marine system. This data set comprises 93 bathymetric surveys along the three submarine channels of the Squamish Delta, British Columbia. These surveys were collected over successive weekdays in the spring and summer of 2011 (Hughes Clarke et al., 2012). Based on changes in seafloor elevation, and direct flow measurements using an acoustic Doppler current profiler, over 100 turbidity currents were recorded in the highly-active proximal channels. However, less than half of these events reached the lobes at the channel mouths (Hughes Clarke et al., 2012; Hizzett et al., 2018; Stacey et al., 2018). We use this unique dataset of closely-spaced repeated surveys to document directly, for the first time, how the stratigraphy of submarine channels is built and preserved at field-scale.

While these data are unusually detailed, we recognize some important caveats in our method and data set. First, the study timescale covers only four months. Hence, we probably do not capture rare but powerful sediment transport events that may decimate the stratigraphic record and cause major topographic modifications (e.g. Strauss and Sadler, 1989; Durkin et al., 2018). Second, repeat surveys should be acquired at a frequency appropriate to the rate of the process being monitored. Hughes Clarke (2016) documented that up to seven turbidity currents may occur within one day. Thus, it is likely that the daily survey repeats may miss some events. Despite these caveats, we know of no other data set that is so detailed (covering the full extent of three channels, with such repetition). We use this exceptionally detailed series of time-lapse bathymetric surveys to understand: (1) how stratigraphy from submarine channels deposits is generated, and (2) the extreme incompleteness of the depositional record, even over a period of just $\sim$4 months.

1.2. Why study the stratigraphic evolution of submarine channel deposits?

Turbidity currents transport sediment from shallow to deep water via submarine channels. As well as carrying globally important volumes of sediment, these flows transport organic carbon, oxygenated waters, nutrients and contaminants that accumulate within submarine channels and downslope at their terminal lobes or submarine fans (Galy et al., 2007; Kao et al., 2010; Gwiazda et al., 2015; Hughes et al., 2015). The often-powerful nature of turbidity currents poses a significant hazard to critical seafloor infrastructure (Carter et al., 2014), which also makes direct monitoring challenging (Inman et al., 1976; Clare et al., 2017). There is a paucity of direct measurements of turbidity currents (Talling et al., 2015), so one typically has to make inferences of past flows based upon the deposits ('turbidites') that are left behind (Hubbard et al., 2014; Jobe et al., 2017). Stratigraphic analysis of turbidites from submarine channels increasingly forms the basis for a wide range of paleo-environment interpretations, including geohazard assessment (Cattaneo et al., 2012), climatic reconstructions (Nakajima and Itaki, 2007), extending historical earthquake catalogues (Bernhardt et al., 2015), and to inform forward stratigraphic modeling for hydrocarbon exploitation (Jobe et al., 2018). Given this importance, it is thus crucial to understand the architecture and completeness of the depositional record for submarine channels. Our study shows how time-lapse bathymetric surveys, allied to sediment cores and monitoring data, can make significant advances in the genesis of deposit architecture.

1.3. Why does stratigraphic completeness matter?

Stratigraphic completeness matters because we need to understand how well deposits can be used to reconstruct sediment transport fluxes, records of geohazards, and to understand the accuracy of numerical models. Stratigraphic completeness is defined here as the proportion of accumulated deposit thickness preserved over a given time period (Sadler, 1981; Strauss and Sadler, 1989). As time increases, the likelihood for preservation of a sedimentary package decreases (Strauss and Sadler, 1989; Fig. 1A), due to short-term autogenic phases of reworking or erosion that follow or intervene phases of deposition, and/or longer-term allogenic factors such as regional subsidence or sea level fluctuations (Barrell, 1917; Paola et al., 2018). Detailed studies of stratigraphic completeness have been performed in fluvial (Reesink et al., 2015; Durkin et al., 2018) and delta-shoreline environments (Straub and Esposito, 2013), but to date no study has attempted to quantify stratigraphic completeness using repeat bathymetric surveys for turbidite systems. Thus, our novel study fills an important knowledge gap and demonstrates the potential for future studies of this type, across a broader range of offshore sedimentary systems.

1.4. Aims

In this study, we analyze the most detailed time-lapse bathymetric surveys yet of any marine system, including turbidite or deltaic systems (Table S1). We combine this with some of the most detailed direct flow monitoring yet conducted (Hughes Clarke, 2016; Hage et al., 2018), and a series of sediment cores ($<$10 m penetration; Hage et al., 2018; Stacey et al., 2018).

Our overarching objective is to document how very frequent time-lapse bathymetric surveys can show (a) how stratigraphic architecture is built, and (b) quantify the incompleteness of that record. We do this over four months for an offshore delta with submarine channels. To address this larger objective, we tackle four specific aims.

First, we show how the stratigraphic architecture of three submarine channels at Squamish Delta is built. We explore how this architecture changes from proximal to distal locations within the channels, and identify how individual stratigraphic elements (i.e. crescentic bedforms, landslide and lobe deposits) are formed and evolve. Second, we determine the stratigraphic completeness of deposits in those three channels following $>$100 turbidity currents over four months. The results are key for interpreting depositional sequences, or informing where sediment cores should be taken to reconstruct flow frequencies and delta history. Third, we seek

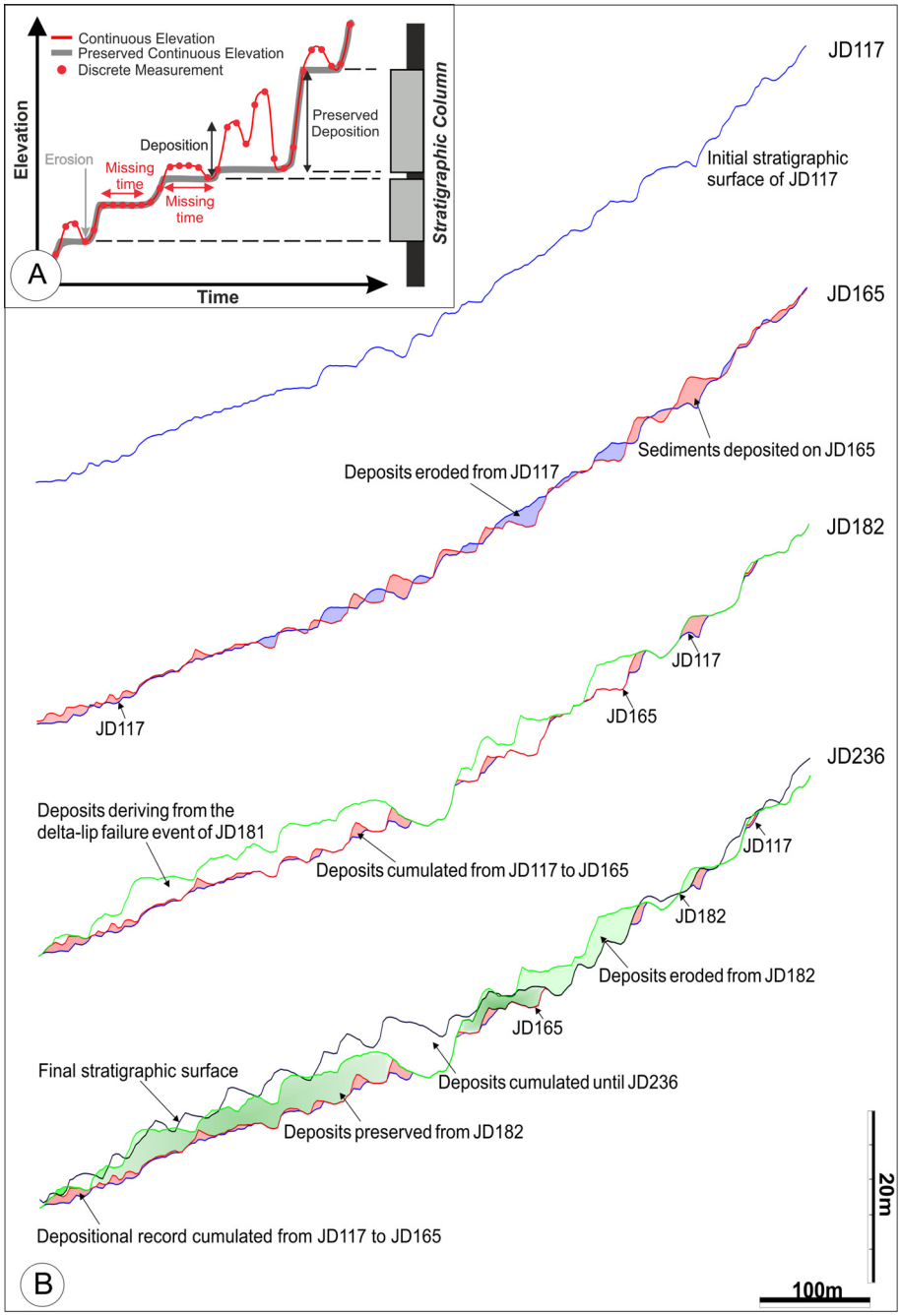

Fig. 1. (A) Schematic diagram illustrating the construction of a stratigraphic column from elevation increments and parameters controlling stratigraphic completeness. Preserved time in stratigraphy is housed in deposits constructed during positive elevation changes that are not later eroded. Gaps in the record occur as a result of stasis on the geomorphic surface and erosion (from Straub and Esposito, 2013). (B) Schematic representation of the algorithm developed to identify the stratigraphic architecture of submarine channel deposits herein studied. JD117 and JD236 are the along channel profiles traced for the first and last bathymetric surveys realized over 4-months period (refer to paragraph 3.2 of the main text). Vertical exaggeration: 8x.

to understand how stratigraphic completeness of three submarine channel deposits varies over the surveyed period, exploring whether occasional large events control the preservation potential of deposits. Finally, we explore how our detailed observations of stratigraphic evolution at an active submarine delta may relate to other deeper-water submarine channel systems.

2. Background: study area and data

The Squamish River carries more than 10^6 m^3 of sediment to its delta annually, where much of that sediment is transported down the submarine prodelta slope by turbidity currents (Hughes Clarke, 2016). Direct monitoring has revealed that >100 turbidity currents may occur during the spring and summer freshet each year, when seasonal meltwater increases the river discharge from ~100 m^3/s in the winter to >500 m^3/s, with peaks of up to 1000 m^3/s (Hughes Clarke et al., 2012). This high frequency turbidity current activity has formed three submarine channels ("northern", "central" and "southern"; Hughes Clarke et al., 2012; Fig. 2A and D). The channels initiate at or very close to the delta-lip, which is partially sub-aerially exposed at low tides. At a distance of ~2 km from the delta-lip, these channels widen and flows become unconfined in water depths of ~150 m (the effective base of the slope; Fig. 2). Recent monitoring has shown that more than two thirds of

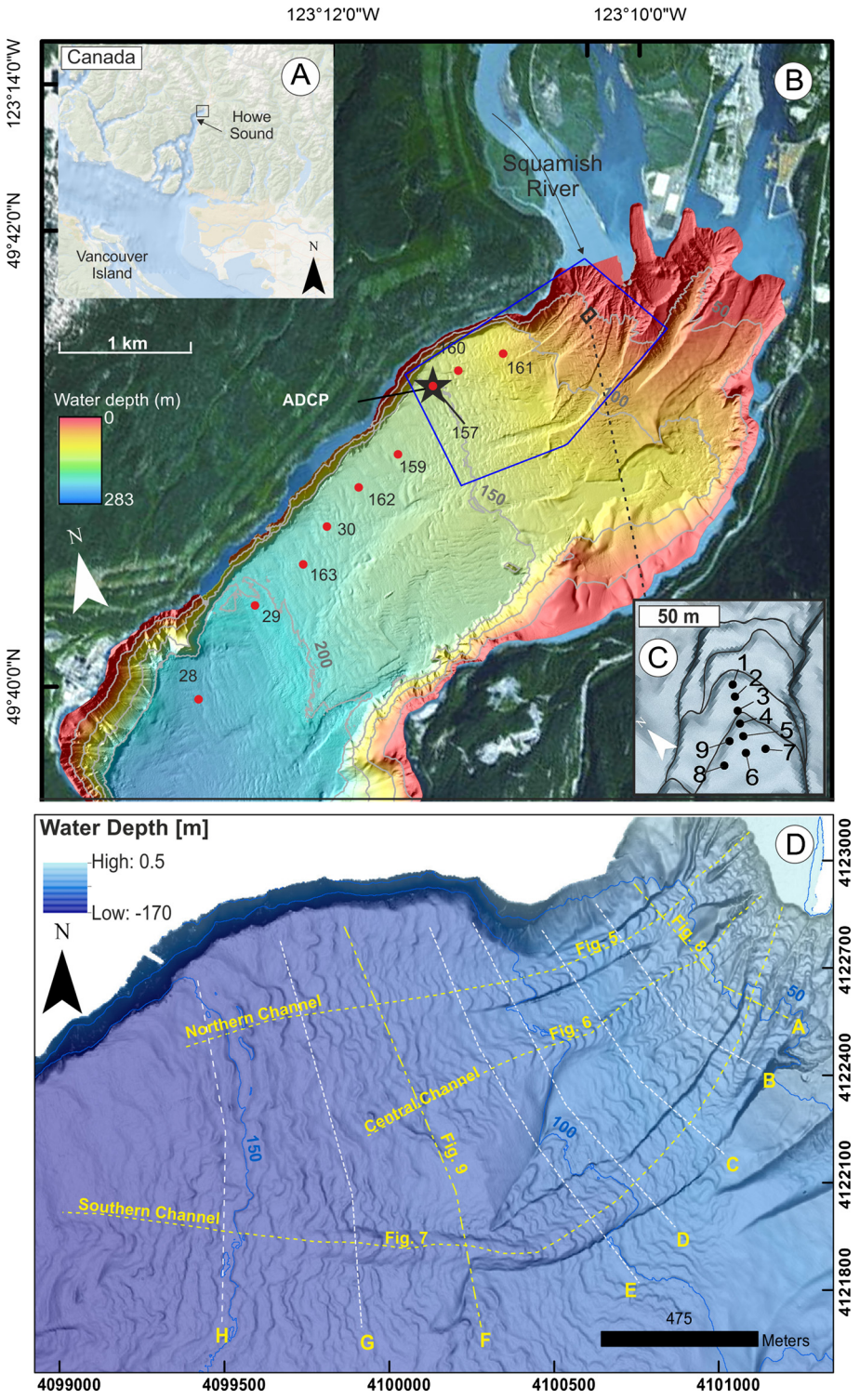

Fig. 2. (A) Location of Squamish Delta in Howe Sound, British Columbia. (B) Location of available sediment cores (red filled circles) from Stacey et al. (2018), ADCP to measure turbidity currents (black star) from Hughes Clarke et al. (2012) and Hughes Clarke (2016), and location of the survey area (blue polygon). (C) Sediment cores from the proximal part of the Central Channel from Hage et al. (2018). (D) In blue extent of area surveyed in 2012 (the focus of this study) annotated with down-channel (northern, central and southern) and cross-channel (A–H) profiles. Selected profiles are shown as figures in this paper (for parts of the down-channel profiles, and cross-channel profiles A and F). All across-channels profiles are available as figures in supplementary material. Animations are also available for all of the profiles as online videos. (For interpretation of the colors in the figure(s), the reader is referred to the web version of this article.)

turbidity currents in these channels are triggered by the settling of sediment from a dilute surface river plume (Hizzett et al., 2018). The other flows are triggered by localized delta-lip collapses (up to 150,000 m^3), which are inferred to result from transient pore pressure changes due to rapid sedimentation and/or tidal fluctuations (Clare et al., 2016).

Detailed multibeam bathymetric surveys were performed on 93 consecutive week days from 17th April 2011 to 24th August 2011, covering an area from the delta top to a distance of ~3,500 m offshore (Hughes Clarke et al., 2012; Fig. 2D). The vertical resolution of these surveys is ~0.1 m, thus it is possible to resolve relatively small changes in seafloor relief between successive surveyed days

(Hizzett et al., 2018). These surveys capture the evolution of three highly active submarine channels at an exceptional level of spatial and temporal detail over four months.

3. Methodology

To quantify stratigraphic completeness at the Squamish Prodelta, we generated maps and profiles from the multibeam bathymetric surveys performed on 93 successive weekdays in 2011. Each daily survey is referred to by the Julian Day (JD) on which it was performed.

3.1. Daily difference maps

We quantified how the seafloor elevation changed by generating *daily difference maps* between pairs of successive surveys (e.g. JD118 minus JD117, JD119 minus JD118) using the same approach as Hizzett et al. (2018). Previous work has shown that the seafloor elevation only changed when a turbidity current or delta-lip failure occurred (Hughes Clarke et al., 2012; Hizzett et al., 2018). In these daily difference maps, negative values represent loss (erosion) and positive values represent sediment accumulation (aggradation). Seafloor changes were detected at the pixel scale, which has a horizontal resolution of 2 m $\times$ 2 m and vertical resolution of approximately 0.1 m (Hughes Clarke et al., 2012; Hizzett et al., 2018). An illustration of how the seafloor level changed with time within the channel axes is presented in supplementary Fig. S1.

3.2. Reconstruction of stratigraphic architecture

We calculated the evolution of *stratigraphic architecture* along eight cross-channel (i.e. along-strike) and three down-channel (i.e. axis-parallel) profiles (Fig. 2D). To do this, we developed an algorithm to build the stratigraphy for each surveyed day along each of those profiles (Fig. 1B). We extracted the bathymetric elevation along each of those profiles for each successive daily survey. Where a point along a profile is higher than it was in the preceding survey (i.e. aggradation occurred), a stratigraphic horizon was created. However, when a point along a profile was lower than it was in the preceding survey (i.e. erosion occurred), the stratigraphy at that point was removed. Each iteration of the algorithm draws all the stratigraphic surfaces traced from the first bathymetric survey until the day that is being processed, accounting for effects of both aggradation and erosion.

Three down-channel (Figs. 5–7) and two across-channel profiles (Figs. 8 and 9) are presented; however, the remaining six along-strike profiles are presented in the supplementary material (Fig. S2–7), as well as accompanying time-lapse movies that visualize the stratigraphic evolution (Movies S1–S18).

3.3. Total difference map

The *total difference map* (Fig. 3A) shows the net thickness of sediments accumulated or eroded over the total surveyed timescale (i.e. JD236 minus JD117). As with the daily difference maps, positive values show where the elevation of the final bathymetric area is higher than the elevation at the start of the survey and indicates net sediment accumulation over the surveyed period. Negative values occur in areas where the final seafloor elevation was lower than at the start.

3.4. Cumulative aggradation map

Turbidity currents deposit, as well as rework sediments emplaced by previous flows; hence, the seafloor may either aggrade or erode at different locations. To create the *cumulative aggradation map* (Fig. 3B), first, we generated the daily difference bathymetric maps. Second, we removed the effect of erosion from each of these daily difference maps by excluding any negative values. In doing so, we only account for the thickness of sediment that would have been deposited at each pixel, had erosion not occurred in the same time period. These positive-value-only difference maps were summed in order to generate the cumulative aggradation map.

Confidence in the multibeam data is lower at the edges of the surveyed areas, where there is no overlap between adjacent swath lines. As a result, the cumulative aggradation map shows artificially higher values at the outer fringes of the survey data. These areas are well outside of the channels, however, and therefore do not affect our analysis.

3.5. Stratigraphic completeness map

The *stratigraphic completeness map* (Fig. 3C) records the ratio between the actual deposit thickness determined over the surveyed period (i.e. the cumulative elevation difference as shown in Fig. 3A) and the total thickness of sediments accumulated over the same time (i.e. the *cumulative aggradation* of sediments shown in Fig. 3B). A value of 1 means that 100% of the sediment deposited at a pixel scale was recorded at the end of the surveyed period. A zero value means that none of the deposited sediment was preserved. The vertical resolution of the multibeam data means that small elevation changes may not be accurately recorded, which can affect our calculations. We determined error ranges following the approach outlined in Hizzett et al. (2018). They determined that during ten days that lacked any turbidity current activity (i.e. when the seafloor was stationary), the distribution of difference map offset values is normally distributed with a mean offset of 4 cm and a standard deviation of 23 cm. In order to model the potential propagated error in our calculations, we added a random value within the range $\pm$4 cm to each pixel of each daily difference map, and each cumulative daily aggradation map. We then recalculated the stratigraphic completeness map from that series of modified maps, and repeated the process a further 99 times. This allows us to understand how confidently we can measure stratigraphic completeness. Based on these calculations, the range in this propagated error for stratigraphic completeness was found to be normally distributed, with a mean of 0.05% and standard deviation of 3% (inset in Fig. 3C).

4. Results

First, we show how stratigraphy is built by submarine flows using 93 time-lapse surveys. We include a brief summary of lithofacies from sediment cores and information from direct monitoring to understand flow types and behavior (Fig. 10). We then document how the stratigraphic completeness of the channels and delta front sequences evolves through time.

4.1. How does the stratigraphic architecture evolve and what elements are involved?

Through the analysis of the daily difference maps and the animations of stratigraphic evolution along 11 profiles (annotated on Fig. 2D, and presented as supplementary movies S1–S18), we identify five distinct stratigraphic elements that make up the stratigraphic architecture developed over the surveyed period. We now discuss these elements in turn.

4.1.1. Crescentic bedforms

The most common differences observed from repeat surveys were up-slope migrating bedforms with a crescentic planform

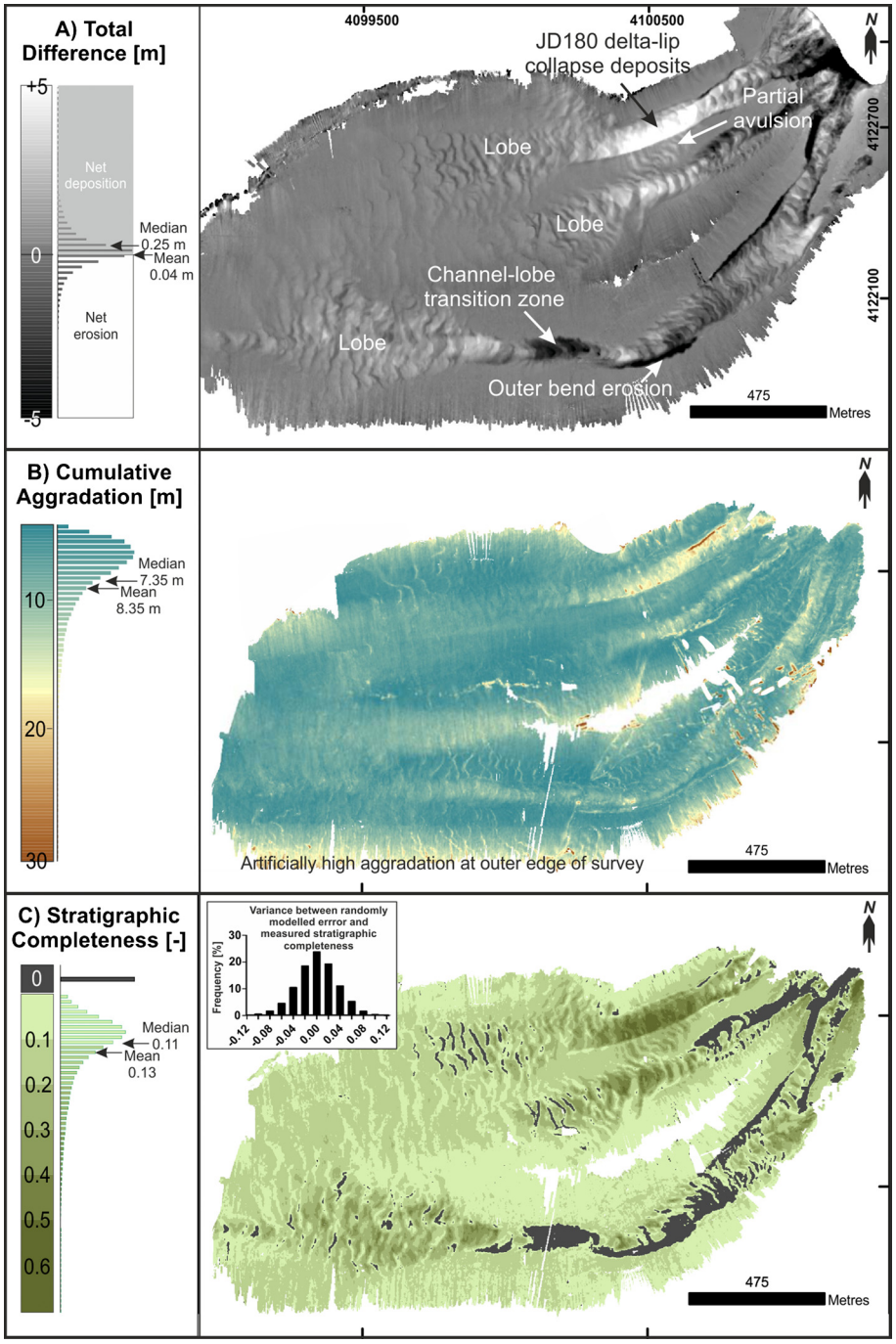

Fig. 3. Generated maps. (A) The Cumulative Elevation Difference Map accounts for the total thickness of sediments at each pixel location at the Squamish prodelta area. Herein, areas with positive values feature deposition, while negative values are related to areas affected by erosion. The Cumulative Aggradation Map (B) shows the aggradation of sediments at each pixel location along the surveyed area. This map does not display the effect of erosion; negative values have, thus, been removed. Artificial over estimation of aggradation is observed at the edges of the surveyed area as a result of non-overlapping swaths of multibeam data. (C) The Stratigraphic Completeness Map shows how complete is the stratigraphic record left behind by multiple turbidity current events. Inset histogram shows the range of error (the bathymetric survey was only realized during weekly day and some days are thus missing, as shown by the white areas of B and C).

(Fig. 2D; Hughes Clarke, 2016; Hage et al., 2018). These bedforms are up to 7 m high with a wavelength of tens of meters, and occur along the axial length of all three of the submarine channels and also on the terminal lobes (Fig. 2D). Thalweg-parallel profiles clearly image erosion on the steep lee sides and deposition on lower angle stoss-sides, which explains their upstream migration (an example is shown in Fig. 6). The upstream migration of bedforms results in the partial, and sometimes entire, reworking of deposits emplaced by previous flows, as an individual bedform trough can migrate a full wavelength in as short a period as two days. This reworking creates a complex final stratigraphy along the channel axis, with a combination of truncated low angle-backsets, bedform remnants and foresets (Figs. 5–7). The crescentic bedforms in the channel axes comprise massive sands that infill complex scours (Hage et al., 2018). The sand is largely ungraded to poorly graded and structureless. Bed thicknesses vary from 1 to 2 m and contacts between layers are sharp and erosive (Fig. 10; Hage et al., 2018). Monitoring using multibeam sonars and acoustic Doppler current profilers show that these bedforms are created by supercritical turbidity currents (1–3 m/s) that undergo repeated

hydraulic jumps (Hughes Clarke, 2016; Hage et al., 2018). Flow acceleration on the lee-sides generally causes erosion, whereas deceleration on the stoss-side promotes deposition (Hughes Clarke, 2016; Hage et al., 2018).

4.1.2. Delta-lip collapse deposits

Five large (up to 150,000 m^3) delta-lip collapses occurred during the surveyed period (Hughes Clarke et al., 2012). The bulk of the run-out from these slope failures is generally limited to the upper and middle sections of the submarine channels, where a considerable thickness of sediment is emplaced en-masse (Fig. 5). The largest delta-lip collapse occurred at the head of the northern channel a few hours after a peak in river discharge (JD180–182), and dramatically changed the channel morphology by plugging its upper reach with ∼5 m of sediments (Fig. 5) (Hughes Clarke et al., 2012). This event effectively filled the proximal part of the channel and triggered a partial avulsion; forming a small splay to the south (Fig. 3A). Within a few days, however, the northern channel adopted a new axis, offset by ∼50 m to the south of the original, incising into the delta-lip collapse deposits (Fig. 8). The thalweg-parallel profile in the upper part of the northern channel also reveals that the delta-lip collapse locally 'smoothed out' the stepped seafloor texture formed by the upstream-migration of bedforms by emplacing a sediment infilling (∼5 m) (Fig. 5 – middle panel). In the days following this event, upstream-migrating bedforms were more elongate and less regular, but ultimately resumed their original morphology and dimensions within a few tens of days (Fig. 5; Movies S1–S3). While not cored here, their deposits likely comprise coarse delta-derived massive or convoluted sand with an erosional base, based on granular slope failures in delta and estuarine settings (van den Berg et al., 2017).

4.1.3. Steep-faced channel-lobe-transition scour zones

Two major erosional events created scour zones, which are clearly observed along the profile that orthogonally transects the southern channel at its transition from the channel to the terminal lobe (Fig. 9). The first occurred on JD180, when the channel base level dropped by ∼5 m. In the following days, 2 m of progressive sediment infill occurred, until JD203 when the axis of the channel vertically incised a further ∼4 m. These two short-lived but significant incisional events ensure that the channel-lobe transition zone of the southern channel is an area of net erosion. Thalweg-parallel profiles reveal that these abrupt and steep-faced erosional features migrated upstream ∼50–100 m in one day (Fig. 7 – bottom panel). No cores have been acquired in these features to date.

4.1.4. Channel margins

In addition to the abrupt lateral offset of channel axes in response to delta-lip collapses (Fig. 5), we also observe lateral migration that does not appear to respond to the emplacement of an obstacle. Two pronounced episodes of lateral axis shifting affected the southern channel during the surveyed period. The first migration occurred between JD158 and JD175 when the channel axis shifted ∼3 m southwards. The second occurred between JD188 and JD189 when the channel axis shifted ∼3 m northwards. It remains in this position until the end of the survey (Fig. 8). Accretion packages formed on the inner side of the channel composed of multiple 0.1–1.5 m-thick beds are dominated by a mixture of coarse- and fine-grained sand at their base with finer grained, less amalgamated beds towards the top (Fig. 10; Hage et al., 2018).

4.1.5. Draped interfluves

Across-slope profiles reveal a steady but low rate of aggradation on the interfluves (Figs. 8–9; see supplementary movies S11–S18). Proximal areas feature ∼1.5 m of aggradation over the survey period, whereas in distal areas up to 5 m of aggradation occurs (Figs. 8–9). Deposits comprise thick silty mud beds interbedded with very thin layers of sand (Fig. 10). Plane-parallel to wavy and sub-parallel laminations are often present, ranging from 1 mm to 1 cm (Hage et al., 2018). The level of daily aggradation on the interfluves is often at, or very close to, the vertical resolution of the multibeam (i.e. <0.1–0.2 m), hence confident identification of internal architecture is not always possible. For this reason, it is also likely that the algorithm we use to build the stratigraphy may overestimate the amount of erosion in these areas of low aggradation outside of the submarine channels and lobes. Thus, we primarily focus our attention on understanding the stratigraphic completeness within and immediately adjacent to the channels and lobes, rather than the interfluves.

4.2. What is the stratigraphic completeness, and how does that vary spatially?

Over the 4-months study period, the median stratigraphic completeness of the area including the three submarine channels is 11% (mean of 13%; Fig. 3). However, there is a large degree of spatial variability, related to the various stratigraphic elements (Figs. 3–4). The three submarine channels also show slightly different patterns of stratigraphic completeness. The extent of areas featuring no preservation of deposits accounts for 4.4% of the total surveyed area (2.6×10^6 m^2).

Northern Channel: The northern channel features the highest stratigraphic completeness proximally, ranging from 35% to 60% (Fig. 3C). These relatively high values are coincident with the run-out extent of major delta-lip failures, which appear to be better preserved compared to the 'background' deposition from repeated turbidity currents. While post-emplacement reworking occurred, much of the delta lip-collapse deposits remain at the end of the survey period.

Central Channel: Since there was no delta-lip failure within the central channel, the overall stratigraphic completeness recorded is much lower than the northern channel. The highest value within the channel is in its medial to distal segments (20–50%; Fig. 3C), while much of its proximal reach was completely eroded (i.e. 0%; Fig. 3C).

Southern Channel: In the southern channel, the stratigraphic completeness varies between 0% and ∼25%. However, at the lobes it reaches values of 40%, and can be as low as zero due to localized erosion on the lee-side of upstream-migrating bedforms (Fig. 7 – bottom panel). In particular, the areas of greatest erosion occur at an outer channel bend and the channel-lobe transition zone, which both yield no stratigraphic record. In these areas, the channel base level was lower at the end of the surveyed period than at the start (Fig. 3C).

4.3. How does stratigraphic completeness vary through time?

The evolution of stratigraphic completeness is demonstrated through time, by presenting an averaged (mean) value for 500 m-long sequential sections along the thalweg-parallel profiles (Fig. S8 from the supplementary material). Following the first pair of daily surveys, stratigraphic completeness quickly drops and assumes values that closely straddle the survey-wide median of 11%, primarily due to the repeated deposition and reworking during upstream-migration of crescentic bedforms. This apparent equilibrium is disrupted on JD181, however; one day after the first significant river flood peak of the freshet (∼900 m^3/s on JD180). In the northern channel, a rapid increase in stratigraphic completeness is documented in the upper 1000 m along its course (up to two times greater in the upper 500 m), which corresponds to the emplacement of the largest delta-lip collapse deposit (150,000 m^3) ob-

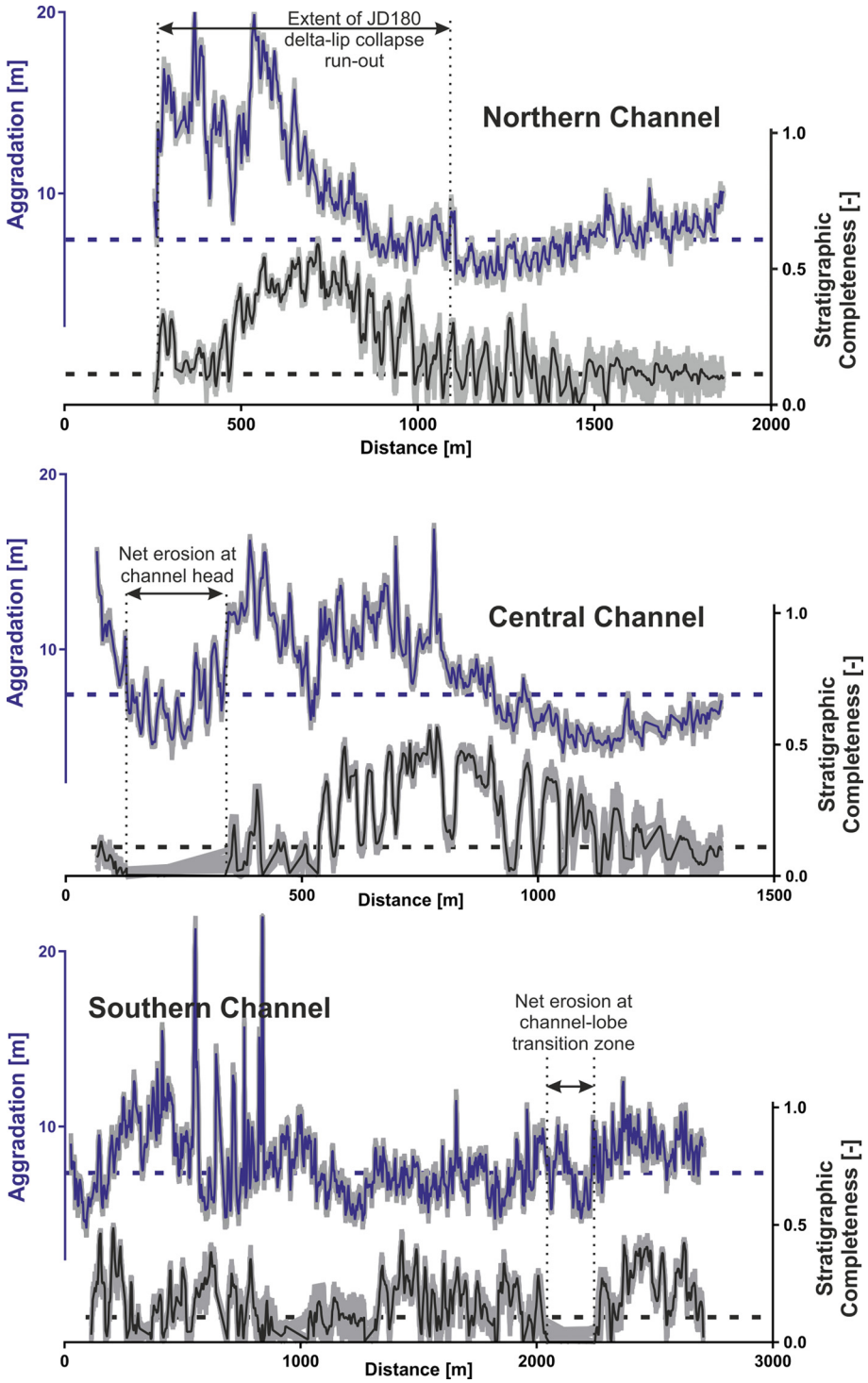

Fig. 4. Error estimation: Thalweg-parallel plots of aggradation and stratigraphic completeness for the three submarine channels. Aggradation is shown in blue, stratigraphic completeness in black, and gray lines represent the error ranges based on random additions of ±5 cm to the seafloor elevation for each survey over 100 runs. Median values for stratigraphic completeness and cumulative aggradation across the surveyed area are shown as dashed lines.

served in the surveyed period (Fig. 4). The central channel shows an increase in stratigraphic completeness between 500 and 1000 m along its course, due to mostly depositional events occurring between JD155 and JD182. At the same time in the southern channel, there is a sudden drop in completeness (mean of 0% between 900 and 1000 m and between 2000 and ∼2300 m down-channel) when channel-filling deposits are flushed down-channel. This decrease in stratigraphic completeness is coincident with the most pronounced period of channel axis incision (Fig. 9). After that point, the stratigraphic completeness appears to more-or-less plateau and reaches a steady state (Fig. 4).

5. Discussion

While the proximal channelized part of the fjord-delta (the focus of our study) features ∼100 turbidity currents per year, much larger, but rarer, events are known from sediment cores in the distal parts of the fjord (Stacey et al., 2018) (Fig. 10). Flows that run

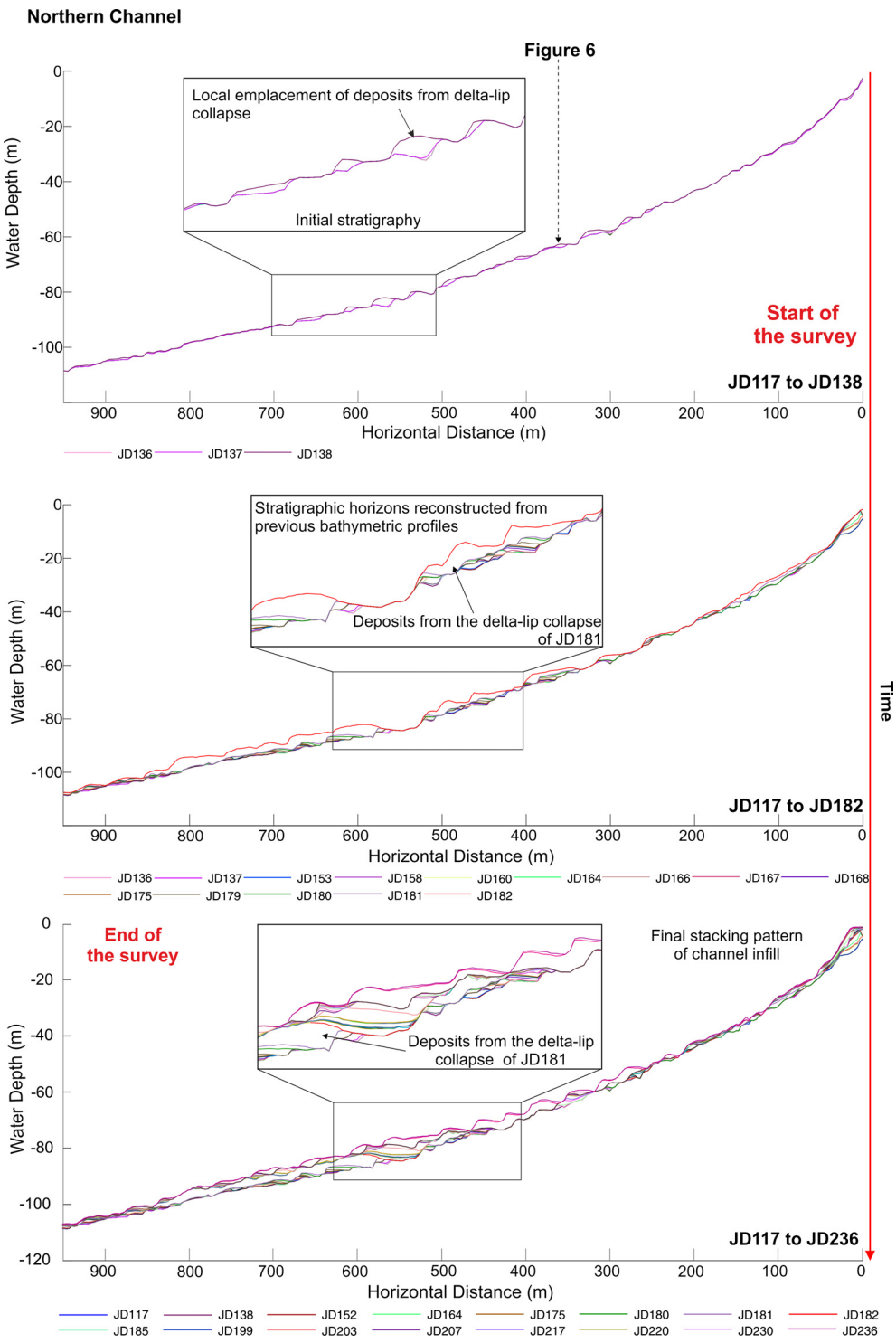

Fig. 5. Down channel profiles of the proximal to medial area of the northern channel generated from the start JD117 (upper panel) to the end of the survey JD236 (bottom panel). The upper panel shows the seafloor at the start of the survey until JD138. The central panel displays the stacking pattern of channel deposits from JD117 to JD182. This includes the major delta-lip failure event occurring between JD181 and JD182 in response to a pick in the river discharge. The bottom panel shows the final stratigraphic architecture of those deposits resulting from >100 turbidity currents events that occurred during 4 months' survey period. Geomorphic surfaces are here represented with single lines color-coded by Julian Day (refer to Fig. 2 for the location of the profile and see animated video Movie S1 to Movie S3 in the supplementary material) (vertical exaggeration: 7x).

~10–15 km further downslope, to the distal fjord basin, have a recurrence of ~100 yr and are not included in our analysis. We must therefore recognize that our study is limited to observing the relatively short-term stratigraphic evolution of the proximal channels and lobes, and the stratigraphy over longer timescales is likely to be even less complete than our data indicate.

5.1. Up-stream migrating bedforms ensure low stratigraphic completeness within submarine channels

The most common sediment transport process at Squamish submarine delta is by Froude-supercritical turbidity currents, which create upstream-migrating bedforms. These flows account for the lee-side erosion and stoss-side deposition observed in the

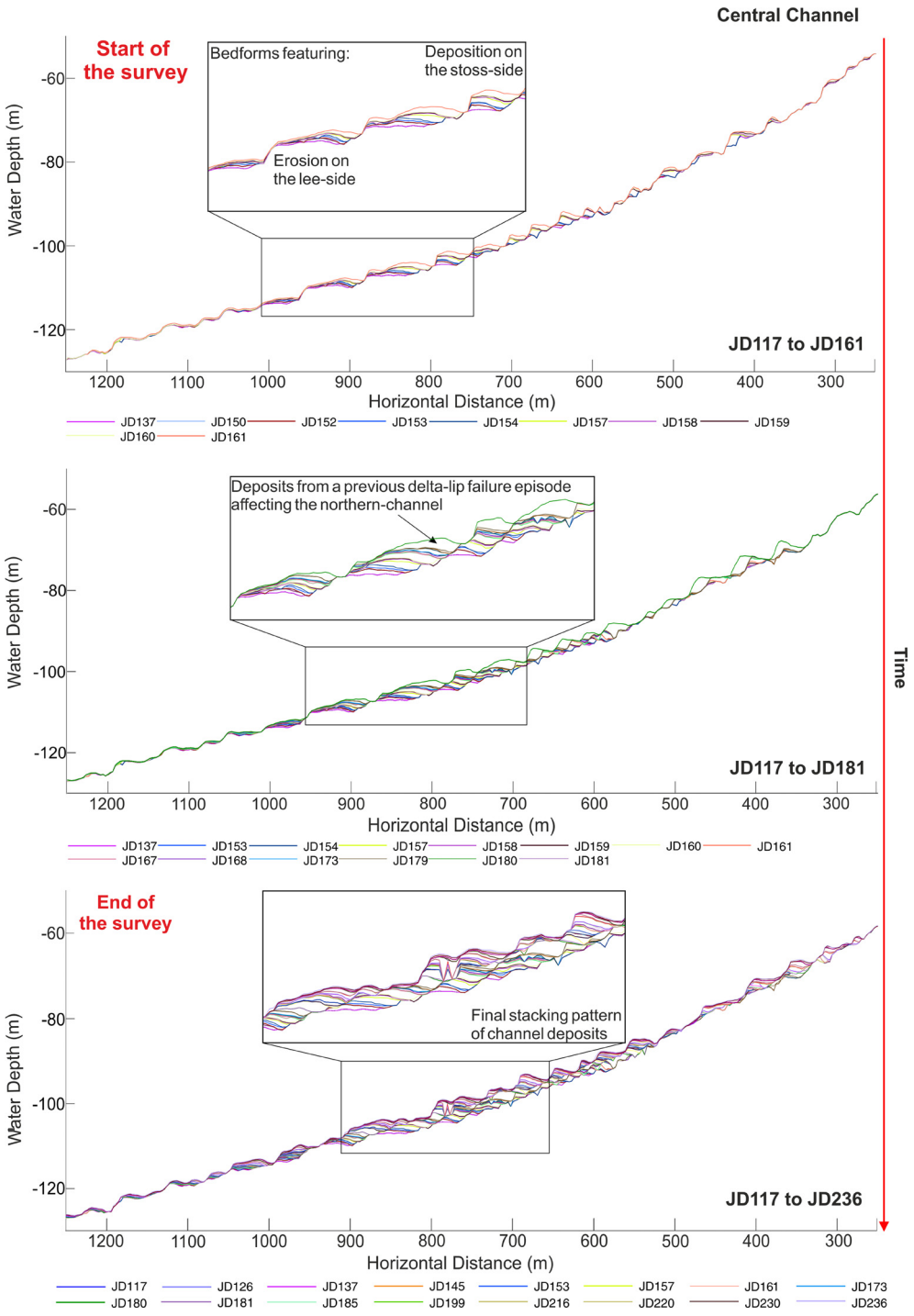

Fig. 6. Along channel profiles of the medial to distal area of the central channel. The upper panel displays the stacking pattern of the submarine channel deposits as consequence of turbidity currents happening between JD117 (start of the survey) and JD161. At the slope breaks upstream migrating bedforms act to both emplace and erode/rework deposits. In the central panel upslope crescentic bedforms feature erosion on the lee-side and deposition on the stoss-side. The bottom panel displays the final stratigraphic architecture of those deposits at the end of the survey JD236. Due to the upper-slope migrating bedforms this area represents the zone of the most intense reworking of sediments. (JD = Julian day, see Fig. 2B for the location of the profile) (vertical exaggeration: 5x).

time-lapse stratigraphic evolution animations (Movies S1–S10), and have been directly monitored by Hughes Clarke (2016). Sequential trains of these upstream-migrating bedforms, interpreted to be formed by a cyclic step instability in the turbidity current, are the dominant feature in many proximal, sandy submarine channels on steep slopes worldwide (Kostic et al., 2010; Symons et al., 2016; Casalbore et al., 2016; Covault et al., 2017; Hage et al., 2018). Upstream-migrating bedforms occur along all reaches of the submarine channels at Squamish, from their mouths to the terminal lobe. By analyzing a small section (over five bedform wavelengths) of the proximal part of the central channel, Hage et al. (2018) showed how deposits of these bedforms may initially be preserved as low-angle back-stepping beds, but that progressive reworking by successive flows may only preserve remnants of the basal scour-fill (Lang et al., 2017; Ono and Björklund, 2018). Low-angle backsets appear to be preserved locally along the three channel axes, from proximal to distal (Figs. 5–7). A further trace of this intense reworking it is also represented by erosional

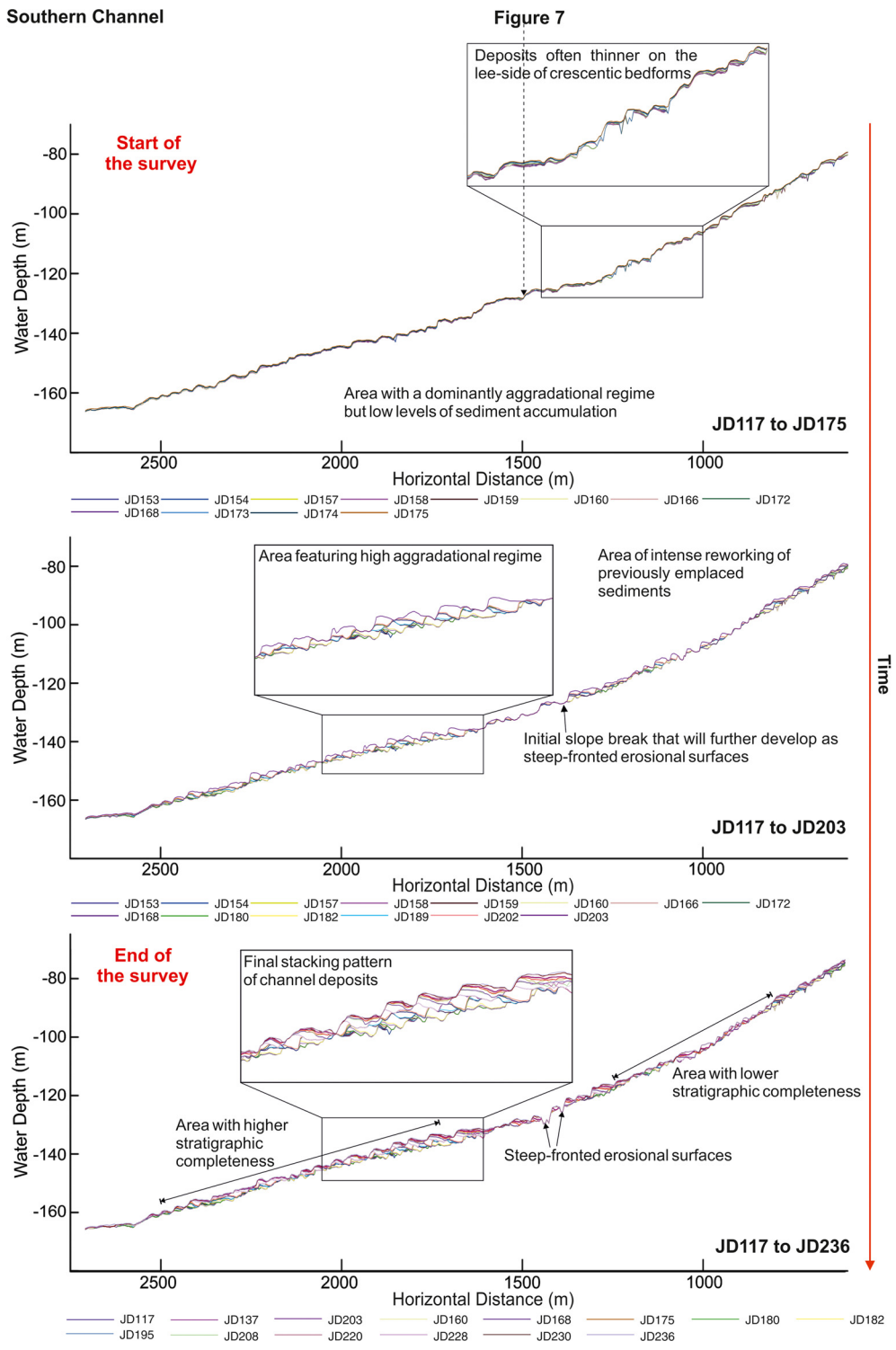

Fig. 7. Along channel profiles at the channel lobe transition zone of the southern channel (see Fig. 2B for their location). The upper panel shows the stratigraphic architecture of submarine channel deposits from the start of the survey JD117 until JD175. The central panel shows the evolution of those bedforms to much more defined features with foreset on the lee-side and more gentle backsets on the stoss-side. The bottom panel displays the final patterns of deposition and erosion of those deposits; herein, sediments are often thinner on the lee-side of crescentic bedforms rather than eroded (vertical exaggeration: 8x).

surfaces visible as possible foresets along the channel lobe transition zone of the southern channel (Fig. 7).

The progressive reworking of previously deposited sediments by successive flows explains the relatively low stratigraphic completeness (Figs. 5–8) of all the three channels axes. Only ~10% of deposit thickness (typically the lowermost scour-fill) is preserved on average due to subsequent reworking. In cases where bedforms migrate upstream faster than the aggradation rate, deposits are entirely obliterated from the stratigraphic record. This is particularly pronounced in the upper reaches of the southern channel that seems to be deepening its course. Stratigraphic completeness is generally much higher at the terminal lobes of all three channels, where flows expand and decelerate (and hence the potential for erosion is lower; Kostic and Parker, 2006). Despite lobe deposits being relatively well preserved, the maximum observed lobe stratigraphic completeness is still only 40%. Therefore, the often-held

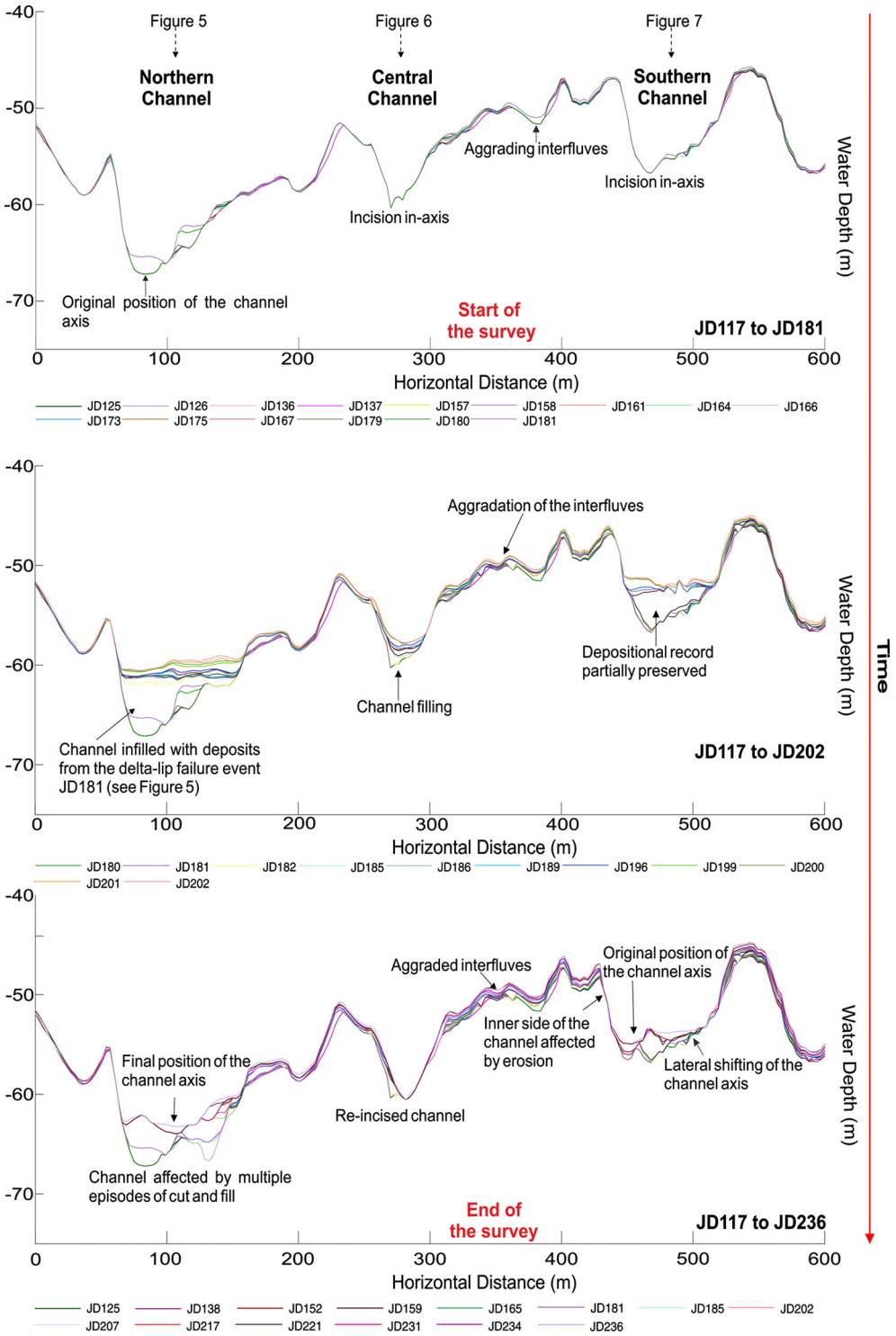

Fig. 8. Cross-channel profiles of the proximal sector of Squamish prodelta (see Fig. 2B, Line A). In this section, the northern and southern channels feature a later migration of their axis, and complex off-axis accumulations. The preservation of depositional records is commonly higher on the interfluves (refer to Fig. 3C) (vertical exaggeration: 14x).

assumption that lobes provide a near-complete stratigraphic record of long run-out flows may not always be valid (Jobe et al., 2018).

5.2. Landslide deposits that modify channel morphology are disproportionately well preserved, but may still be extensively reworked over longer timescales

The highest stratigraphic completeness within the channels corresponds to areas with the highest aggradation. In the most extreme case, the high aggradation within channels relates to en-masse emplacement of 150,000 m^3 of sediments following a delta-lip collapse event on JD180 at the head of the northern channel (and not a cyclic step process) (Fig. 5). This sudden deposition of sediment fundamentally changed channel morphodynamics by 'smoothing out' the relief of crescentic bedforms and effectively plugging the channel, and triggering a partial avulsion (Fig. 3A). Similar observations of subaqueous landslides modifying channel morphology and turbidity currents pathways have been made in

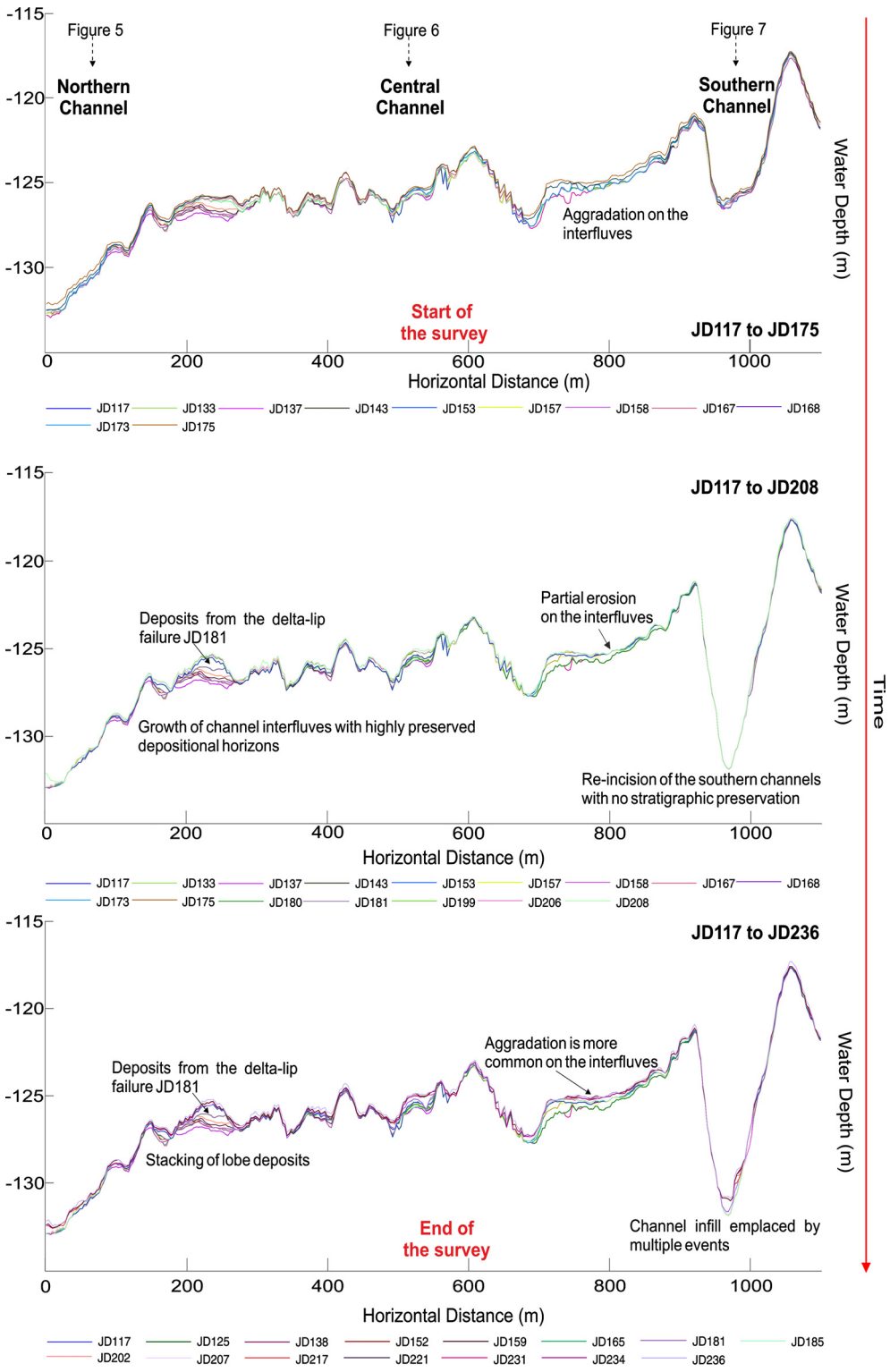

Fig. 9. Cross-profiles of the distal area (see Fig. 2B, Line F). Temporal evolution of the distal sector of the prodelta area. Preservation of the depositional records mainly affects the interfluves and aggrading levees. The southern channel features multiple episodes of channel filling and cut off the stratigraphic records (refer to the main test) (vertical exaggeration: 21x).

deep-sea (Armitage et al., 2009; Brooks et al., 2017) and lacustrine settings (Corella et al., 2016). The stratigraphic completeness in the proximal part of the northern channel is anomalously high compared with the other channels. This high completeness corresponds to the run-out extent of the JD180 delta-lip failure; hence, it appears that slope failures, for which the majority of their volume is not transformed into a turbidity current (i.e. a landslide), are preserved in the depositional record (at least over the surveyed timescale). However, at least 64% of the landslide mass was subsequently reworked by repeated turbidity currents, which ultimately incised a new channel axis into its deposits (Fig. 8). This is similar to observations from other repeat surveys, such as in Monterey Canyon, California, where 80% of an emplaced landslide volume was removed by turbidity currents over less than

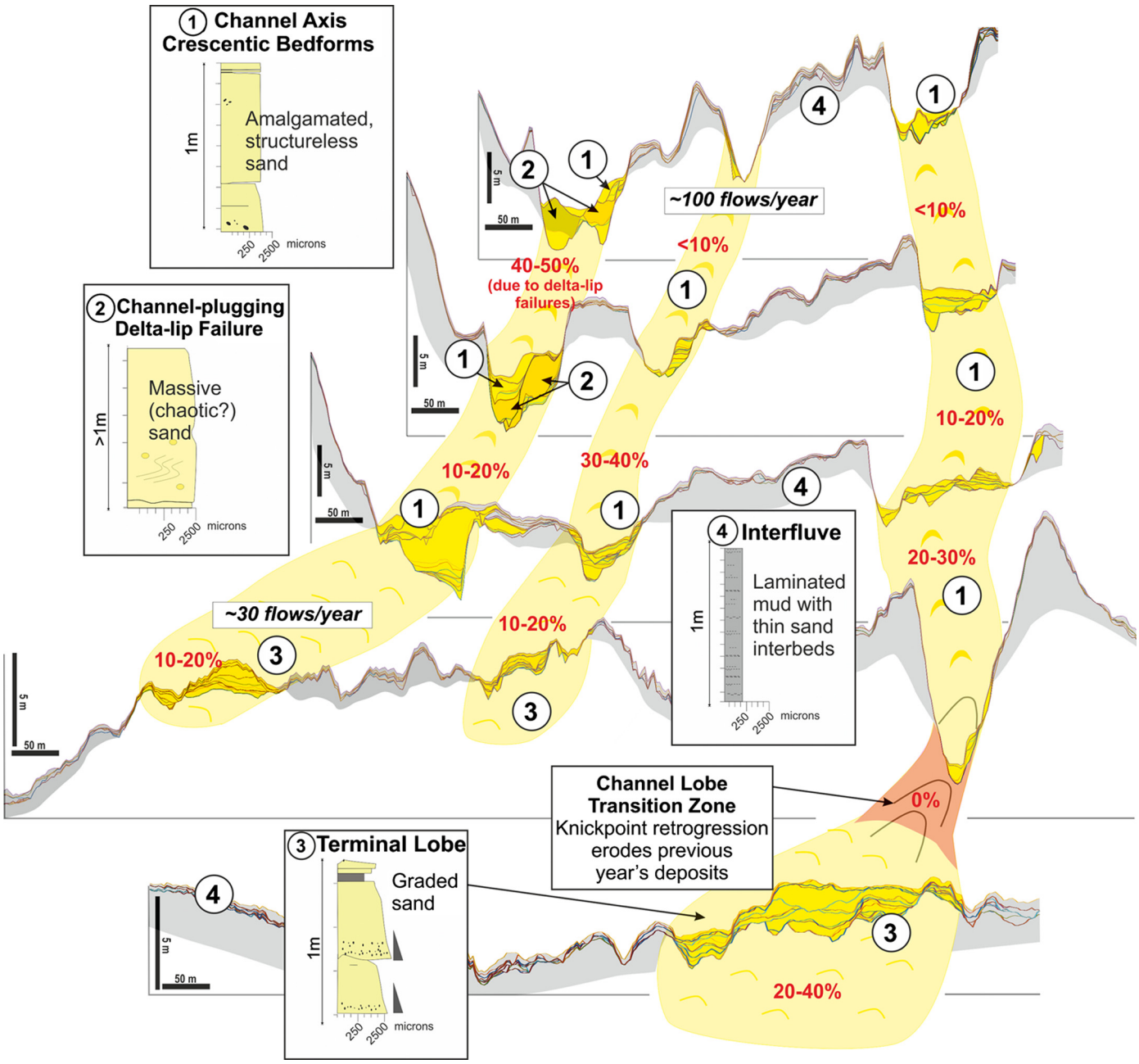

Fig. 10. Correlation of submarine channel deposits with their resultant stratigraphic architecture across the surveyed area. Black numbers recall the depositional facies of the sediments cores used to reconstruct this section. Red numbers refer to the completeness of the stratigraphic records from the proximal to the distal area. Flow frequency is also estimated from higher at the channels head to lower at the channels mouth (vertical exaggeration 10x).

two years (Smith et al., 2007). Biscara et al. (2012) suggested that the entirety of a landslide deposit may be reworked by frequent turbidity currents, based on repeat surveys at the Ogooué Delta, Gabon. Reconstruction of landslide frequency and volume in submarine channels may therefore be challenging when analyzing outcrops, seismic data and sediment cores and significant post-emplacement reworking has occurred.

5.3. The most incomplete records result from short-lived and infrequent erosive events

Two short-lived erosional events were responsible for not only the removal of deposits accumulated at the channel-lobe transition of the southern channel during 2011, but also incision into deposits from previous years (Fig. 9). Up to 5 m of vertical erosion occurred, with 200 m of retrogression, which is clearly shown by a sudden drop in the averaged stratigraphic completeness in the southern channel (between ~800 and 1,400 m down-channel of Fig. 4) on JD181 (Fig. 3). At several time-steps, these features resemble steep-fronted erosional steps in rivers known as knickpoints that may be triggered by changes in the base level (Crosby and Whipple, 2006; Gales et al., 2018) (video S9 and S10). These scours may form in a similar manner, as progradation of the lobe could have a similar effect to the base level change in a river. If the southern channel extends seaward, for instance, then the present day channel lobe-transition zone may become a site of backfilling, or back stepping and deposition, while the focus of erosion will advance down-slope (Hamilton et al., 2013).

5.3.1. Why is stratigraphic completeness so low at the channel-lobe transition?

Stratigraphic completeness at this channel-lobe transition is zero, and may be explained by the strengthening of the erosional capacity that the most powerful flows have at the exit of channel confinement (Kostic and Parker, 2006; Covault et al., 2017; Dorrell et al., 2016). Mega-scours have been observed at similar transitional points at several sites in the deep sea (Wynn et al., 2002); hence such areas should be expected to have very low stratigraphic completeness (Mutti and Normark, 1987; Macdonald et al., 2011). These two major incisional events were also coincident with flushing of much of the previously accumulated sediment from the upper reaches of the southern channel, and the lateral erosion at the outer channel bend. Such channel-incising events represent ∼2% of the total number of events occurring during the surveyed period, compared to ∼98% that fill the channel, but appear to be strong controls on stratigraphic completeness. These events have the potential to remove significant thicknesses of sediment, and thus erase several years of sediment accumulation in locations such as the channel lobe transition zone (Conway et al., 2012). The location of the channel lobe transition zone may change over time as the channel evolves through developing slope breaks that can migrate up or down-stream and will consequently influence successive flows (Fig. 9). Such events are perhaps more important for sculpting the geometry of channels and dictating what will ultimately be preserved over geologic timescales, than the more frequent flows that form upstream-migrating bedforms.

5.3.2. Do the powerful erosive events relate to an exceptional trigger?

It has been suggested that powerful triggers are required for channel-incising events, such as major earthquakes, extreme river floods or sea level change (Canals et al., 2006; Piper and Normark, 2009). The timing of the first channel-incising event is closely associated with the first major river flood discharge peak of the year, hence a sudden seaward flushing of delta-top sediments may be responsible (Clare et al., 2016); however, the specific cause for the second is unclear. It is plausible that once sufficient sediment had accumulated within the upper reaches of the channel, a 'normal' turbidity current was able to bulk up through entrainment of freshly deposited sediment, and 'ignite', without needing an exceptional trigger (Pantin, 1979; Parker, 1982; Hizzett et al., 2018).

5.4. How do our findings relate to other systems worldwide?

It is important to understand the wider implications of our results at Squamish Delta for interpreting submarine channel deposit geometries and completeness more generally. Currently, there are no comparably detailed time-lapse bathymetric datasets available, however. This makes it impossible to make direct comparisons to similar data from other sites. We thus first discuss whether the morphological features seen at Squamish Delta (e.g. crescentic bedforms) are found in other proximal sandy submarine or sublacustrine channels. If they are, then results from Squamish Delta can form part of more general models. We then discuss morphologies of muddier submarine channel systems.

5.4.1. Implications for other sandy submarine channels

Similar-scale upstream-migrating bedforms have been observed from repeat seafloor surveys of sandy proximal submarine channels in lakes (Fricke et al., 2015), estuarine settings (Normandeau et al., 2014), submarine deltas (Conway et al., 2012; Casalbore et al., 2017), deep-sea canyons (Smith et al., 2005, 2007; Paull et al., 2018) and volcanic islands (Chiocci et al., 2013; Casalbore et al., 2014; Clare et al., 2018). The repetition of erosion and deposition that occurs during the upstream-migration of these crescentic bedforms ensures that the stratigraphic completeness of the submarine channel deposits will be low in these highly active and bypass-dominated settings. Such sandy-floored channels may therefore be relatively poor for reconstructing event-histories (particularly where aggradation rates are low), and can render core-to-core correlation impossible, even within distances of a few tens of meters (Hage et al., 2018).

5.4.2. Implications for larger muddy submarine channels

Similar scale upstream-migrating bedforms do not appear to typify larger mud-dominated systems. However, longer wavelength (c. 500 m) bedforms that are inferred to have migrated upstream have been observed in sites such as the deep-sea Amazon Fan (Normark et al., 2002). As the resolution of bathymetric data is a function of water depth, it is possible that this has precluded identification of bedforms in most deep-water sites (Symons et al., 2016). Thus, it is unclear as to precisely how well our findings may relate to the world's largest muddy submarine channels (e.g. Amazon, Indus and Congo).

Recent direct monitoring of turbidity currents in the upper reaches of the offshore Congo Canyon, demonstrated that subannually-recurring turbidity currents are capable of eroding seafloor sediment, which is then transported further down-canyon (Azpiroz-Zabala et al., 2017). Comparison of this flow monitoring data with sediments acquired from seafloor coring indicated that the depositional record under-represents the frequency of turbidity currents by at least an order of magnitude in the axis of the muddy Congo Canyon. In similarly-active muddy systems, stratigraphic completeness is thus unlikely to be high in the channel axis, but how this varies across and down the system is also unclear. Until high-resolution time-lapse data are available, we hypothesize that accumulation of mud may shield underlying deposits from subsequent erosion, and that areas of low stratigraphic completeness may be less extensive in muddy systems. This may promote a higher stratigraphic completeness than that observed in proximal sandy settings, such as at Squamish Delta. This current uncertainty underlines the need for more repeat seafloor surveys in a wider range of active settings in order to better constrain the relative controls played by substrate, system scale and aggradation rate on stratigraphic completeness.

6. Conclusions

We report one of the most detailed time-lapse studies of any turbidity current system. Through combining flow monitoring, repeat bathymetric surveys and core sampling, we revealed how three active submarine channels build stratigraphic architecture. In this setting, the effects of upstream-migrating bedforms ensure that stratigraphic completeness is generally low (even in the terminal lobes of the system), because of the competing effects of deposition and erosion. Other less-frequent events, such as delta-lip collapses and incision at the down-slope transition to the lobe, can exert a more profound influence on what is recorded in the depositional record (or not). Short lived, more powerful and infrequent events can exert varied effects: delta-lip collapses may be largely preserved, while canyon-flushing flows may remove significant thicknesses of sediment. These insights into the stratigraphic completeness of active submarine channels demonstrate that one should expect a high degree of incompleteness in similar systems. Frequency of flows, aggradation rate and the extent of variation in magnitude of events all play important roles and dictate exactly how incomplete the ultimate geological record will be. Perhaps most importantly, we have demonstrated how repeat surveys can be used to monitor the stratigraphic evolution of submarine systems. The emergence of autonomous survey platforms now enables multiple repeat, high resolution surveys, requiring limited human

effort, and opens up exciting new opportunities to understand how a much wider range of offshore systems evolve and provide calibration for numerical models.

Acknowledgements

Vendettuoli is funded by Natural Environment Research Council (NERC) CASE Award NE/L009358/1 “First high resolution direct measurements for powerful turbidity currents that reach the deep ocean”. In particular, we thank the captain and surveyors aboard the CSL Heron. We acknowledge NERC funding (NE/M007138/1, NE/M017540/1, NE/P009190/1, NE/P005780/1). Clare acknowledges support from NERC National Capability project Climate Linked Atlantic Sector Science (CLASS). We thank the Editor, Jean-Philippe Avouac, Daniele Casalbore and Zane Jobe for their insightful reviews, which improved the final paper.

Appendix A. Supplementary material

Supplementary material related to this article can be found online at https://doi.org/10.1016/j.epsl.2019.03.033.

References

Armitage, D.A., Romans, B.W., Covault, J.A., Graham, S.A., 2009. The influence of mass-transport-deposit surface topography on the evolution of turbidite architecture: the Sierra Contreras, Tres Pasos Formation (Cretaceous), southern Chile. J. Sediment. Res. 79 (5), 287–301.

Azpiroz-Zabala, M., Cartigny, M.J., Talling, P.J., Parsons, D.R., Sumner, E.J., Clare, M.A., Simmons, S.M., Cooper, C., Pope, E.L., 2017. Newly recognized turbidity current structure can explain prolonged flushing of submarine canyons. Sci. Adv. 3 (10), e1700200.

Barrell, J., 1917. Rhythms and the measurements of geologic time. Bull. Geol. Soc. Am. 28 (1), 745–904.

Bernhardt, A., Melnick, D., Hebbeln, D., Lückge, A., Strecker, M.R., 2015. Turbidite paleoseismology along the active continental margin of Chile–Feasible or not? Quat. Sci. Rev. 120, 71–92.

Biscara, L., Hanquiez, V., Leynaud, D., Marieu, V., Mulder, T., Gallissaires, J.M., Garlan, T., 2012. Submarine slide initiation and evolution offshore Pointe Odden, Gabon—analysis from annual bathymetric data (2004–2009). Mar. Geol. 299, 43–50.

Brooks, H.L., Hodgson, D.M., Brunt, R.L., Peakall, J., Flint, S.S., 2017. Exhumed lateral margins and increasing flow confinement of a submarine landslide complex. Sedimentology. https://doi.org/10.1111/sed.12415.

Canals, M., Puig, P., de Madron, X.D., Heussner, S., Palanques, A., Fabres, J., 2006. Flushing submarine canyons. Nature 444 (7117), 354.

Carter, L., Gavey, R., Talling, P.J., Liu, J.T., 2014. Insights into submarine geohazards from breaks in subsea telecommunication cables. Oceanography 27 (2), 58–67.

Casalbore, D., Chiocci, F.L., Scarascia Mugnozza, G., Tommasi, T., Sposato, A., 2011. Flash-flood hyperpycnal flows generating shallow-water landslides at Fiumara mouths in Western Messina Strait (Italy). Mar. Geophys. Res. 27 (32), 257.

Casalbore, D., Romagnoli, C., Bosman, A., Chiocci, F.L., 2014. Large-scale seafloor waveforms on the flanks of insular volcanoes (Aeolian Archipelago, Italy), with inferences about their origin. Mar. Geol. 355, 318–329.

Casalbore, D., Bosman, A., Ridente, D., Chiocci, F., 2016. Coastal and submarine landslides in the tectonically-active Tyrrhenian Calabrianmargin (Southern Italy): examples and geohazard implications. In: Krastel, S. (Ed.), Submarine Mass Movements and Their Consequences. In: Advances in Natural and Technological Hazards Research, vol. 37. Springer, Heidelberg, pp. 261–269.

Casalbore, D., Ridente, D., Bosman, A., Chiocci, F.L., 2017. Depositional and erosional bedforms in Late Pleistocene–Holocene pro-delta deposits of the Gulf of Patti (southern Tyrrhenian margin, Italy). Mar. Geol. 385, 216–227.

Cattaneo, A., Babonneau, N., Ratzov, G., Dan-Unterseh, G., Yelles, K., Bracène, R., et al., 2012. Searching for the seafloor signature of the 21 May 2003 Boumerdès earthquake offshore central Algeria. Nat. Hazards Earth Syst. Sci. 12 (7), 2159–2172.

Chiocci, F.L., et al., 2013. Bathy-morphological setting of Terceira Island (Azores) after the FAIVI cruise. J. Maps 9 (4), 590–595.

Clare, M.A., Clarke, J.H., Talling, P.J., Cartigny, M.J.B., Pratomo, D.G., 2016. Preconditioning and triggering of offshore slope failures and turbidity currents revealed by most detailed monitoring yet at a fjord-head delta. Earth Planet. Sci. Lett. 450, 208–220.

Clare, M., Vardy, M., Cartigny, M., Talling, P., Himsworth, M., Dix, J., Belal, M., 2017. Direct monitoring of active geohazards: emerging geophysical tools for deep-water assessments. Near Surf. Geophys. 15 (4), 427–444.

Clare, M., Le Bas, T., Price, D., Hunt, J., Sear, D., Cartigny, M., Vellinga, A., Symons, W., Firth, C., Cronin, S., 2018. Complex and cascading triggering of submarine landslides and turbidity currents at volcanic islands revealed from integration of high-resolution onshore and offshore surveys. Front. Earth Sci. https://doi.org/10.3389/feart.2018.00223.

Clark, J.D., Pickering, K.T., 1996. Architectural elements and growth patterns of submarine channels: application to hydrocarbon exploration. Am. Assoc. Pet. Geol. Bull. 80 (2), 194–220.

Conway, K.W., Barrie, J.V., Picard, K., Bornhold, B.D., 2012. Submarine channel evolution: active channels in fjords, British Columbia, Canada. Geo Mar. Lett. 32 (4), 301–312.

Corella, J.P., Loizeau, J.L., Kremer, K., Hilbe, M., Gerard, J., Le Dantec, N., Girardclos, S., 2016. The role of mass-transport deposits and turbidites in shaping modern lacustrine deepwater channels. Mar. Pet. Geol. 77, 515–525.

Covault, J.A., Kostic, S., Paull, C.K., Sylvester, Z., Fildani, A., 2017. Cyclic steps and related supercritical bedforms: building blocks of deep-water depositional systems, western North America. Mar. Geol. 393, 4–20.

Crosby, B.T., Whipple, K.X., 2006. Knickpoint initiation and distribution within fluvial networks: 236 waterfalls in the Waipaoa River, North Island, New Zealand. Geomorphology 82 (1–2), 16–38.

Dorrell, R.M., Peakall, J., Sumner, E.J., Parsons, D.R., Darby, S.E., Wynn, R.B., et al., 2016. Flow dynamics and mixing processes in hydraulic jump arrays: implications for channel-lobe transition zones. Mar. Geol. 381, 181–193.

Durkin, P.R., Hubbard, S.M., Holbrook, J., Boyd, R., 2018. Evolution of fluvial meander-belt deposits and implications for the completeness of the stratigraphic record. Geol. Soc. Am. Bull. 130 (5–6), 721–739. https://doi.org/10.1130/B31699.1.

Fricke, A.T., Sheets, B.A., Nittrouer, C.A., Allison, M.A., Ogston, A.S., 2015. An examination of Froude-supercritical flows and cyclic steps on a subaqueous lacustrine delta, Lake Chelan, Washington, USA. J. Sediment. Res. 85 (7), 754–767.

Gales, J.A., Talling, P.J., Cartigny, M.J., Hughes Clarke, J., Lintern, G., Stacey, C., Clare, M.A., 2018. What controls submarine channel development and the morphology of deltas entering deep-water fjords? Earth Surf. Process. Landf. https://doi.org/10.1002/esp.4515.

Galy, V., France-Lanord, C., Beyssac, O., Faure, P., Kudrass, H., Palhol, F., 2007. Efficient organic carbon burial in the Bengal fan sustained by the Himalayan erosional system. Nature 450 (7168), 407.

Gwiazda, R., Paull, C.K., Ussler III, W., Alexander, C.R., 2015. Evidence of modern fine-grained sediment accumulation in the Monterey Fan from measurements of the pesticide DDT and its metabolites. Mar. Geol. 363, 125–133.

Hage, S., Cartigny, M.J.B., Clare, M.A., Sumner, E.J., Vendettuoli, D., Hughes Clarke, J.E., Hubbard, S.M., Talling, P.J., Lintern, D.G., Stacey, C.D., Englert, R.G., Vardy, M.E., Hunt, J.E., Yokokawa, M., Parsons, D.R., Hizzett, J.L., Azpiroz-Zabala, M., Vellinga, A.J., 2018. How to recognize crescentic bedforms formed by supercritical turbidity currents in the geologic record: insights from active submarine channels. Geology. https://doi.org/10.1130/G40095.1.

Hamilton, P.B., Strom, K., Hoyal, D.C., 2013. Autogenic incision-backfilling cycles and lobe formation during the growth of alluvial fans with supercritical distributaries. Sedimentology 60 (6), 1498–1525.

Hill, P.R., Conway, K., Lintern, D.G., Meulé, S., Picarda, K., Barriea, J.V., 2008. Sedimentary processes and sediment dispersal in the southern Strait of Georgia, BC, Canada. Mar. Environ. Res. 66 (Supplement), S39–S48.

Hizzett, J.L., Hughes Clarke, J.E., Sumner, E.J., Cartigny, M.J.B., Talling, P.J., Clare, M.A., 2018. Which triggers produce the most erosive, frequent, and longest runout turbidity currents on deltas? Geophys. Res. Lett. 45 (2), 855–863.

Hubbard, S.M., Covault, J.A., Fildani, A., Romans, B.W., 2014. Sediment transfer and deposition in slope channels: deciphering the record of enigmatic deep-sea processes from outcrop. Geol. Soc. Am. Bull. 126 (5–6), 857–871.

Hughes, D.J., Shimmield, T.M., Black, K.D., Howe, J.A., 2015. Ecological impacts of large-scale disposal of mining waste in the deep sea. Sci. Rep. 5, 9985. https://doi.org/10.1038/srep09985.

Hughes Clarke, J.E., 2016. First wide-angle view of channelized turbidity currents links migrating cyclic steps to flow characteristics. Nat. Commun. 7, 11896.

Hughes Clarke, J.E., Brucker, S., Muggah, J., Hamilton, T., Cartwright, D., Church, I., Kuus, P., 2012. Temporal progression and spatial extent of mass wasting events on the Squamish prodelta slope. In: Landslides and Engineered Slopes: Protecting Society Through Improved Understanding. Taylor and Francis Group, London, pp. 1091–1096.

Inman, D.L., Nordstrom, C.E., Flick, R.E., 1976. Currents in submarine canyons: an air-sea-land interaction. Annu. Rev. Fluid Mech. 8 (1), 275–310.

Jobe, Z., Sylvester, Z., Pittaluga, M.B., Frascati, A., Pirmez, C., Minisini, D., Cantelli, A., 2017. Facies architecture of submarine channel deposits on the western Niger Delta slope: implications for grain-size and density stratification in turbidity currents. J. Geophys. Res., Earth Surf. 122 (2). https://doi.org/10.1002/2016JF003903.

Jobe, Z.R., Howes, N., Romans, B.W., Covault, J.A., 2018. Volume and recurrence of submarine-fan-building turbidity currents. Depositional Rec. 4 (2), 160–176. https://doi.org/10.1002/dep2.42.

Kao, S.J., Dai, M., Selvaraj, K., Zhai, W., Cai, P., Chen, S.N., Syvitski, J.P., 2010. Cyclone-driven deep sea injection of freshwater and heat by hyperpycnal flow in the subtropics. Geophys. Res. Lett. 37 (21).

Kelner, M., Migeon, S., Tric, E., Couboulex, F., Dano, A., Lebourg, T., 2016. Frequency and triggering of small-scale submarine landslides on decadal timescales: analysis of 4D bathymetric data from the continental slope offshore Nice (France). Mar. Geol. 379, 281–297.

Kostic, S., Parker, G., 2006. The response of turbidity currents to a canyon–fan transition: internal hydraulic jumps and depositional signatures. J. Hydraul. Res. 44 (5), 631–653.

Kostic, S., Sequeiros, O., Spinewine, B., Parker, G., 2010. Cyclic steps: a phenomenon of supercritical shallow flow from the high mountains to the bottom of the ocean. J. Hydro-Environ. Res. 3 (4), 167–172.

Lang, J., Brandes, C., Winsemann, J., 2017. Erosion and deposition by supercritical density flows during channel avulsion and backfilling: field examples from coarse-grained deepwater channel-levée complexes (Sandino Forearc Basin, southern Central America). Sediment. Geol. 349, 79–102.

Lintern, D.G., Hill, P.R., Stacey, C., 2016. Powerful unconfined turbidity current captured by cabled observatory on the Fraser River delta slope, British Columbia, Canada. Sedimentology 63 (5), 1041–1064.

Macdonald, H.A., Wynn, R.B., Huvenne, V.A., Peakall, J., Masson, D.G., Weaver, P.P., McPhail, S.D., 2011. New insights into the morphology, fill, and remarkable longevity (>0.2 my) of modern deep-water erosional scours along the northeast Atlantic margin. Geosphere 7 (4), 845–867.

Mastbergen, D., van den Ham, G., Cartigny, M., Koelewijn, A., de Kleine, M., Clare, M., 2016. Multiple flow slide experiment in the Westerschelde Estuary, The Netherlands. In: Submarine Mass Movements and Their Consequences. Springer International Publishing, pp. 241–249.

Moody, J.A., Meade, R.H., 2014. Ontogeny of point bars on a river in a cold semi-arid climate. Bull. Geol. Soc. Am. 126 (9–10), 1301–1316. https://doi.org/10.1130/B30992.1.

Mountjoy, J.J., Howarth, J.D., Orpin, A.R., Barnes, P.M., Bowden, D.A., Rowden, A.A., Schimel, A.C.G., Holden, C., Horgan, H.J., Nodder, S.D., Patton, J.R., Lamarche, G., Gerstenberger, M., Micallef, A., Pallentin, A., Kane, T., 2018. Earthquakes drive large-scale submarine canyon development and sediment supply to deep-ocean basins. Sci. Adv. 4, eaar3748.

Mutti, E., Normark, W.R., 1987. Comparing examples of modern and ancient turbidite systems: problems and concepts. In: Marine Clastic Sedimentology. Springer, Dordrecht, pp. 1–38.

Nakajima, T., Itaki, T., 2007. Late Quaternary terrestrial climatic variability recorded in deep-sea turbidites along the Toyama Deep-Sea Channel, central Japan Sea. Palaeogeogr. Palaeoclimatol. Palaeoecol. 247 (1–2), 162–179.

Normandeau, A., Lajeunesse, P., St-Onge, G., Bourgault, D., Drouin, S.S.O., Senneville, S., Bélanger, S., 2014. Morphodynamics in sediment-starved inner-shelf submarine canyons (Lower St. Lawrence Estuary, Eastern Canada). Mar. Geol. 357, 243–255.

Normark, W.R., Piper, D.J., Posamentier, H., Pirmez, C., Migeon, S., 2002. Variability in form and growth of sediment waves on turbidite channel levees. Mar. Geol. 192 (1–3), 23–58.

Ono, K., Björklund, P., 2018. Froude supercritical flow bedforms in deepwater slope channels? Field examples in conglomerates, sandstones and fine-grained deposits. Sedimentology 65 (3), 639–669.

Pantin, H.M., 1979. Interaction between velocity and effective density in turbidity flow: phase-plane analysis, with criteria for autosuspension. Mar. Geol. 31 (1–2), 59–99.

Paola, C., Straub, K., Mohrig, D., Reinhardt, L., 2009. The "unreasonable effectiveness" of stratigraphic and geomorphic experiments. Earth-Sci. Rev. 97 (1–4), 1–43.

Paola, C., Ganti, V., Mohrig, D., Runkel, A.C., Straub, K.M., 2018. Time not our time: physical controls on the preservation and measurement of geologic time. Annu. Rev. Earth Planet. Sci. 46, 409–438.

Paull, C.K., Talling, P.J., Maier, K.L., Parsons, D., Xu, J., Caress, D.W., Gwiazda, R., Lundsten, E.M., Anderson, K., Barry, J.P., Chaffey, M., et al., 2018. Powerful turbidity currents driven by dense basal layers. Nat. Commun. 9 (1), 4114.

Parker, G., 1982. Conditions for the ignition of catastrophically erosive turbidity currents. Mar. Geol. 46 (3–4), 307–327.

Piper, D.J., Normark, W.R., 2009. Processes that initiate turbidity currents and their influence on turbidites: a marine geology perspective. J. Sediment. Res. 79 (6), 347–362.

Reesink, A.J.H., Van den Berg, J.H., Parsons, D.R., Amsler, M.L., Best, J.L., Hardy, R.J., Szupiany, R.N., 2015. Extremes in dune preservation: controls on the completeness of fluvial deposits. Earth-Sci. Rev. 150, 652–665.

Sadler, P.M., 1981. Sediment accumulation rates and the completeness of stratigraphic sections. J. Geol. 89 (5), 569–584.

Schwenk, J., Khandelwal, A., Fratkin, M., Kumar, V., Foufoula-Georgiou, E., 2017. High spatiotemporal resolution of river planform dynamics from Landsat: the RivMAP toolbox and results from the Ucayali River. Earth Space Sci. 4 (2), 46–75. Retrieved from http://doi.wiley.com/10.1002/2016EA000196.

Silva, T.A., Girardclos, S., Stutenbecker, L., Bakker, M., Costa, A., Schlunegger, F., Lane, S.N., Molnar, P., Loizeau, J.-L., 2018. The sediment budget and dynamics of a delta-canyon-lobe system over the Anthropocene timescale: the Rhone River Delta, Lake Geneva (Switzerland/France). Sedimentology. https://doi.org/10.1111/sed.12519.

Smith, D.P., Ruiz, G., Kvitek, R., Iampietro, P.J., 2005. Semiannual patterns of erosion and deposition in upper Monterey Canyon from serial multibeam bathymetry. Geol. Soc. Am. Bull. 117 (9), 1123. Retrieved from http://gsabulletin.gsapubs.org/cgi/doi/10.1130/B25510.

Smith, D.P., Kvitek, R., Iampietro, P.J., Wong, K., 2007. Twenty-nine months of geomorphic change in upper Monterey Canyon (2002–2005). Mar. Geol. 236 (1–2), 79–94.

Stacey, C.D., Hill, P.H., Talling, P.J., Enkin, R.J., Hughes Clarke, J., Lintern, D.G., 2018. How turbidity currents frequency and character varies down a delta-fjord system: combining direct monitoring, deposits and seismic data. Sedimentology. https://doi.org/10.1111/sed.12488.

Straub, K.M., Esposito, C.R., 2013. Influence of water and sediment supply on the stratigraphic record of alluvial fans and deltas: process controls on stratigraphic completeness. J. Geophys. Res., Earth Surf. 118 (2), 625–637.

Strauss, D., Sadler, P.M., 1989. Stochastic models for the completeness of stratigraphic sections. Math. Geol. 21 (1), 37–59.

Sylvester, Z., Pirmez, C., Cantelli, A., 2011. A model of submarine channel-levee evolution based on channel trajectories: implications for stratigraphic architecture. Mar. Pet. Geol. 28 (3), 716–727. Retrieved from https://dx.doi.org/10.1016/j.marpetgeo.2010.05.012.

Symons, W.O., Sumner, E.J., Talling, P.J., Cartigny, M.J., Clare, M.A., 2016. Large-scale sediment waves and scours on the modern seafloor and their implications for the prevalence of supercritical flows. Mar. Geol. 371, 130–148.

Talling, P.J., Allin, J., Armitage, D.A., Arnott, R.W., Cartigny, M.J., Clare, M.A., Hill, P.R., 2015. Key future directions for research on turbidity currents and their deposits. J. Sediment. Res. 85 (2), 153–169.

Van den Berg, J.H., Martinius, A.W., Houthuys, R., 2017. Breaching-related turbidites in fluvial and estuarine channels: examples from outcrop and core and implications to reservoir models. Mar. Pet. Geol. 82, 178–205.

Wynn, R.B., Piper, D.J., Gee, M.J., 2002. Generation and migration of coarse-grained sediment waves in turbidity current channels and channel–lobe transition zones. Mar. Geol. 192 (1–3), 59–78.

Xu, J.P., Wong, F.L., Kvitek, R., Smith, D.P., Paull, C.K., 2008. Sandwave migration in Monterey Submarine Canyon, Central California. Mar. Geol. 248, 193–212.